of Combustion Instability in Hybrid Combustion," NASA 1-7310, Sept. 1969, Stanford Research Inst., Menlo Park, Calif., pp. 2–23.

[3] Marxman, G. A. and Woolridge, C. E., "Researches on the Combustion Mechanism of Hybrid Rockets," *Advances in Tactical Rocket Propulsion*, edited by S. S. Penner, AGARD, 1968, Pt. 3, Chap. 1, pp. 425–477.

[4] Houser, T. J., "Kinetics of Polymer from Surface Regression Rates," *Journal of Chemical Physics*, Vol. 45, No. 3, Aug. 1966, pp. 1031–1037.

[5] Rabinovitch, B., "Regression Rates and the Kinetics of Polymer Degradation," *Proceedings of the Tenth Symposium (International)*, Combustion Institute, Pittsburgh, Pa., 1965, pp. 1395–1404.

[6] Rastogi, R. P. and Gupta, B. L., "Combustion Mechanism of Solid Rocket Propellants," *AIAA Journal*, Vol. 7, No. 3, March 1969, pp. 541–542.

[7] Krishnamurthy, L. and Williams, F. A., "On the Temperatures of Regressing PMMA Surfaces," *Combustion and Flame*, Vol. 20, 1973, pp. 163–169.

[8] Baijal, S. K., "Combustion Studies on Boron Containing Polymers," Ph.D. thesis, Jan. 1970, Univ. of Gorakhpur, Gorakhpur, India.

Necessary Condition for Piecewise Uniform Optimum Design under Frequency Constraint

Alain Cardou*
Université Laval, Québec, Canada

Introduction

We have shown in a recent Note,[1] how the piecewise uniform minimum weight of a clamped bar could be obtained exactly for any chosen fundamental frequency of axial vibration. It was also shown that the continuous optimum design can be approximated as closely as desired by using an appropriate number of uniform regions. Since it is desirable from a practical point of view to use as few steps as possible, the objective of this Note is to show the minimum number of steps one must use in order to obtain a given fundamental frequency.

We use here the same notation as in Ref. 1, and the reader should refer to this Note for the derivation of the equations. However, we assume now that the n uniform regions have the same length $L_i = L/n$ (Fig. 1), the frequency parameters α_i all being equal to $\alpha = \beta L/n$. Besides, the only nonstructural mass M is located at the bar tip.

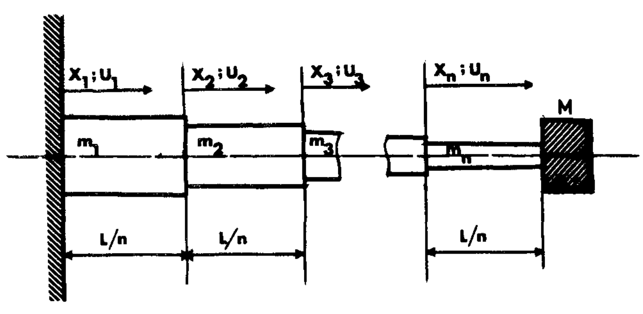

Fig. 1 Clamped bar with n uniform elements.

Received January 18, 1974; revision received May 1, 1974.
Index categories: Structural Dynamic Analysis; Optimal Structural Design.

* Assistant Professor, Department of Mechanical Engineering.

Relation between Frequency and Number of Steps

To obtain information about α, we must eliminate the Lagrange multipliers from Eqs. (7–10) of Ref. 1. Elimination of λ_{i-1} from the last two leads to relation

$$\lambda_i = l\sin^2(\alpha+\Phi_i)/\sin\alpha\cos(\alpha+2\Phi_i) \quad (i = 2,\ldots,n) \qquad (1)$$

which, combined with λ_{i-1}, from Eq. (10), Ref. 1, requires that Φ_i and Φ_{i-1} satisfy

$$\cot\Phi_i = [\sin\alpha\sin(\alpha+\Phi_{i-1}) \pm \cos\Phi_{i-1}]/\cos\alpha\sin(\alpha+\Phi_{i-1}) \quad (i = 3,\ldots,n) \qquad (2)$$

Since $0 < \Phi_i < \pi/2$, the plus sign must be chosen in Eq. (2). This, together with special consideration of the case $i = 2$, (with $\Phi_i = 0$) leads to the alternate recurrence relations

$$\cot\Phi_i = \tan\alpha + 1/(\sin\alpha\cos\alpha + \cos^2\alpha\tan\Phi_{i-1}) \quad (i = 2,\ldots,n) \qquad (3)$$

If $0 < \alpha < \pi/2$, we see from Eq. (3) that

$$\cot\Phi_i > \tan\alpha \quad (i = 2,\ldots,n)$$

Therefore, $\Phi_i + \alpha < \pi/2$, which is the condition to have the first mode. Thus, the only condition in order to get the required fundamental frequency with a given number of steps n is that

$$\alpha = \beta L/n < \pi/2 \qquad (4)$$

Equation (4) shows that for a given number of steps n, the maximum frequency factor obtainable is

$$\beta L \leqq n\pi/2$$

Conversely, if we require a frequency factor βL, we need a minimum number of steps: $n > 2\beta L/\pi$. In particular, as we might expect, a uniform member, $n = 1$, has a maximum $\beta L = \pi/2$.

References

[1] Cardou, A., "Piecewise Uniform Optimum Design for Axial Vibration Requirement," *AIAA Journal*, Vol. 11, No. 12, Dec. 1973, pp. 1760–1761.

Exact and Approximate Analyses of Transient Wave Propagation in an Anisotropic Plate

C. T. Sun*
Purdue University, W. Lafayette, Ind.
AND
R. Y. S. Lai†
University of Wisconsin—Milwaukee, Milwaukee, Wisc.

Introduction

Most of the simplified theories for plates are constructed based on the assumption that the characteristic length of deformation is much larger than the thickness of the structure. The conventional approach in determining the region of adequacy of the plate theories has been by the use of comparing the dispersion curves for the harmonic wave propagation in the plate obtained from the plate theories and the three-

Received January 21, 1974; revision received April 12, 1974. This research was sponsored by the Air Force Materials Laboratory, Wright-Patterson Air Force Base, under Contract F33615-72-C-2113.
Index categories: Structural Composite Materials; Structural Dynamic Analysis.

* Associate Professor, School of Aeronautics and Astronautics. Member AIAA.

† Assistant Professor, Department of Energetics.

dimensional theory of elasticity, respectively. The classical plate theory based on the Kirchhoff hypothesis is generally agreed to be accurate if the wavelength is about ten times the thickness. The Timoshenko type of plate theories which include transverse shear and rotatory inertia are believed to be valid for very short wavelengths for the lowest mode of flexural waves. It is also well known that the Timoshenko type of plate theories, even though very good for the first flexural mode, cannot describe accurately the higher modes of wave propagation. Theoretically, higher order plate theories can be derived by using the power series expansion about the thickness coordinate as suggested by Cauchy and extended later by Mindlin.[1] However, the improvement obtained by retaining more terms in the expansion is at the expense of the desired simplicity of the plate theory.

While being rather comfortable with the application of the plate theories in static problems, natural vibrations, and harmonic wave propagations, we are still uncertain about their usefulness in dealing with the impact problems. Indeed, when a plate is subjected to an impulsive load, reflections of waves from the top and bottom surfaces cannot be accounted for by the plate theories. In addition, higher modes and short wavelength disturbances may be induced.

Because of the increasing use of laminated composites in the turbine blades in the jet engine, damages resulting from the impact of a foreign object have become of great concern. The actual failure process is still unclear and may not be simple in nature. However, it is in general agreed that the cause of the sudden failure must be examined from the point of transient wave propagation phenomena.[2-4]

In this Note, transient waves in a plate of fiber-reinforced composite materials subjected to lateral impulsive loadings are investigated. The unidirectionally reinforced composite is considered as a homogeneous and orthotropic medium. Complex Fourier transform and Laplace transform are employed in the analysis. The inversion of the transforms is done by the use of a computational algorithm, the fast Fourier transform (FFT).

Exact Analysis

Consider an infinite elastic layer reinforced by unidirectional fibers. The layer will be considered effectively as a homogeneous orthotropic elastic medium. The axes x, y, z are taken to coincide with the axes of orthotropy with the x-axis parallel to the fibers. If a state of plane strain parallel to the x-z plane is assumed, the equations of motion can be written as

$$c_{11}\frac{\partial^2 u}{\partial x^2}+c_{55}\frac{\partial^2 u}{\partial z^2}+\frac{\partial^2 w}{\partial x\,\partial z}(c_{13}+c_{55})=\rho\frac{\partial^2 u}{\partial t^2} \tag{1}$$

$$(c_{13}+c_{55})\frac{\partial^2 u}{\partial x\,\partial z}+c_{55}\frac{\partial^2 w}{\partial x^2}+c_{33}\frac{\partial^2 w}{\partial z^2}=\rho\frac{\partial^2 w}{\partial t^2} \tag{2}$$

where u and w are the displacements in the x- and z-directions, respectively; ρ is the mass density; and c_{ij} are the elastic constants.

Equations (1) and (2) can be nondimensionalized as

$$c_{11}{}^*\frac{\partial^2 U}{\partial X^2}+c_{55}{}^*\frac{\partial^2 U}{\partial Z^2}+(c_{13}{}^*+c_{55}{}^*)\frac{\partial^2 W}{\partial X\,\partial Z}=\frac{\partial^2 U}{\partial T^2} \tag{3}$$

$$(c_{13}{}^*+c_{55}{}^*)\frac{\partial^2 U}{\partial X\,\partial Z}+c_{55}{}^*\frac{\partial^2 W}{\partial X^2}+c_{33}{}^*\frac{\partial^2 W}{\partial Z^2}=\frac{\partial^2 W}{\partial T^2} \tag{4}$$

in which

$$\begin{gathered}U=u/h,\quad W=w/h,\quad X=x/h,\quad Z=z/h\\ T=t(G_{TT}h/\rho)^{1/2},\quad c_{ij}{}^*=c_{ij}/G_{TT}\end{gathered} \tag{5}$$

where h is the thickness of the layer, and $G_{TT}=c_{44}$ is the transverse shear rigidity in the y-z plane.

We denote the Fourier transform and Laplace transform by

$$\bar{f}(s)=\int_{-\infty}^{\infty}f(X)e^{-isX}\,dX \tag{6}$$

and

$$\bar{f}(p)=\int_{0}^{\infty}f(T)e^{-pT}\,dT \tag{7}$$

respectively. Taking the transforms of Eqs. (3) and (4) we obtain

$$-(p^2+c_{11}{}^*s^2)\tilde{\bar{U}}+c_{55}{}^*\frac{d^2\tilde{\bar{U}}}{dZ^2}+(c_{13}{}^*+c_{55}{}^*)is\frac{d\tilde{\bar{W}}}{dZ}=0 \tag{8}$$

$$-(c_{55}{}^*s^2+p^2)\tilde{\bar{W}}+c_{33}{}^*\frac{d^2\tilde{\bar{W}}}{dZ^2}+(c_{55}{}^*+c_{13}{}^*)is\frac{d\tilde{\bar{U}}}{dZ}=0 \tag{9}$$

Equations (8) and (9) can be solved for $\tilde{\bar{W}}$ and $\tilde{\bar{U}}$. We obtain for $\tilde{\bar{W}}$

$$\tilde{\bar{W}}=C_1e^{\alpha_1Z}+C_2e^{\alpha_2Z}+C_3e^{\alpha_3Z}+C_4e^{\alpha_4Z} \tag{10}$$

where C_i are integration constants, and α_i are the roots of the characteristic equation

$$H_1\alpha^4-H_2\alpha^2+H_3=0 \tag{11}$$

in which the coefficients are given by

$$\begin{aligned}H_1&=c_{33}{}^*c_{55}{}^*\\ H_2&=c_{55}{}^*(c_{55}{}^*s^2+p^2)+c_{33}{}^*(p^2+c_{11}{}^*s^2)-(c_{13}{}^*+c_{55}{}^*)^2s^2\\ H_3&=(c_{55}{}^*s^2+p^2)(p^2+c_{11}{}^*s^2)\end{aligned} \tag{12}$$

The solution for $\tilde{\bar{U}}$ can be obtained easily from Eqs. (8) and (9).

The transformed nondimensional stress components can be easily shown to be

$$\tilde{\bar{\sigma}}_{zz}{}^*=c_{13}{}^*is\tilde{\bar{U}}+c_{33}{}^*d\tilde{\bar{W}}/dZ \tag{13}$$

$$\tilde{\bar{\sigma}}_{xz}{}^*=c_{55}{}^*[(d\tilde{\bar{U}}/dZ)+is\tilde{\bar{W}}] \tag{14}$$

where

$$\sigma_{zz}{}^*=\sigma_{zz}/G_{TT},\quad \sigma_{xz}{}^*=\sigma_{xz}/G_{TT} \tag{15}$$

It is assumed that the upper surface of the plate is subjected to an impulsive line load q while the bottom surface remains free from tractions. The boundary conditions can be nondimensionalized and transformed into

$$\tilde{\bar{\sigma}}_{zz}{}^*=\tilde{\bar{q}}^*,\quad \tilde{\bar{\sigma}}_{xz}{}^*=0,\quad Z=0.5 \tag{16}$$

$$\tilde{\bar{\sigma}}_{zz}{}^*=\tilde{\bar{\sigma}}_{xz}{}^*=0,\quad Z=-0.5 \tag{17}$$

where

$$q^*=q/G_{TT} \tag{18}$$

Substitution of Eqs. (13) and (14), in conjunction with the solutions for $\tilde{\bar{W}}$ and $\tilde{\bar{U}}$, into Eqs. (16) and (17) leads to

$$\begin{bmatrix}F_1e^{\alpha_1}&F_2e^{\alpha_2}&F_3e^{\alpha_3}&F_4e^{\alpha_4}\\ G_1e^{\alpha_1}&G_2e^{\alpha_2}&G_3e^{\alpha_3}&G_4e^{\alpha_4}\\ F_1&F_2&F_3&F_4\\ G_1&G_2&G_3&G_4\end{bmatrix}\begin{bmatrix}C_1\\C_2\\C_3\\C_4\end{bmatrix}=\begin{bmatrix}\tilde{\bar{q}}^*\\0\\0\\0\end{bmatrix} \tag{19}$$

where

$$F_j=\alpha_j[c_{33}{}^*DE-B_2c_{13}{}^*c_{55}{}^*s-D^2c_{13}{}^*s]/DE\,e^{\alpha_j/2} \tag{20}$$

$$G_j=(B_j+sD)/D\,e^{\alpha_j/2} \tag{21}$$

$$B_j=c_{33}{}^*\alpha_j{}^2-(c_{55}{}^*s^2+p^2) \tag{22}$$

$$D=(c_{55}{}^*+c_{13}{}^*)s \tag{23}$$

$$E=(p^2+c_{11}{}^*s^2) \tag{24}$$

The integration constants C_j ($j=1$–4) thus can be determined from Eq. (19). Inversion is now the remaining work.

Solution by Plate Theory

The plate equations for fiber-reinforced composite plates developed by Whitney and Pagano[5] will be employed. Using the same coordinate system as described previously, the equations of motion for the plate in a state of plane strain parallel to the x-z plane are

$$\kappa A_{55}\left(\frac{\partial\psi_x}{\partial x}+\frac{\partial^2 w^0}{\partial x^2}\right)+q=\rho h\frac{\partial^2 w^0}{\partial t^2} \tag{25}$$

$$D_{11}\frac{\partial\psi_x}{\partial x^2}-\kappa A_{55}\left(\psi_x+\frac{\partial w^0}{\partial x}\right)=\rho I\frac{\partial^2\psi_x}{\partial t^2} \tag{26}$$

where w^0 is the transverse displacement, ψ_x is the rotation of the plane section perpendicular to the x-axis, $\kappa(=\pi^2/12)$ is a shear correction factor, and A_{55} and D_{11} are the plate transverse-shear and plate bending rigidities, respectively. (For details of the plate equations, see Ref. 5.)

Equations (25) and (26) can be again nondimensionalized and then transformed. The transformed equations are

$$(p^2+\kappa A_{55}{}^*s^2)\tilde{\bar{W}}^0-\kappa A_{55}{}^*is\tilde{\bar{\psi}}_x=\tilde{\bar{q}}^* \tag{27}$$

$$\kappa A_{55}{}^*is\tilde{\bar{W}}^0+(I^*p^2+D_{11}{}^*s^2+\kappa A_{55}{}^*)\tilde{\bar{\psi}}_x=0 \tag{28}$$

where the dimensionless quantities are defined as

$$W^0=w^0/h,\quad I^*=I/h^3,\quad A_{55}{}^*=A_{55}/G_{TT}h,\quad D_{11}{}^*=D_{11}/G_{TT}h^3 \tag{29}$$

Solving Eqs. (27) and (28), we obtain

$$\tilde{\bar{W}}^0=\tilde{\bar{q}}^*/\beta \tag{30}$$

where

$$\beta=(p^2+\kappa A_{55}{}^*s^2)-\kappa^2A_{55}{}^{*2}s^2/(I^*p^2+D_{11}{}^*s^2+\kappa A_{55}{}^*) \tag{31}$$

Numerical Inversion by FFT

The inversions of the transformed solutions given by Eqs. (10) and (30) are carried out numerically by use of the fast Fourier transform method.[6] The fast Fourier transform method is a computational algorithm with which inversions of the Fourier transform and, with a slight change of variables, the Laplace transform can be computed on digital computers.[7,8] It is found in the following numerical examples that the computing time for the exact solution is significantly longer than that for the plate solution.

The material chosen for the numerical examples is the boron-epoxy composite for which a typical set of material constants are given by

$$E_L=25\times10^6\text{ psi},\quad E_T=1\times10^6\text{ psi},\quad \nu_{TT}=\nu_{LT}=0.25$$
$$G_{LT}=0.5\times10^6\text{ psi},\quad G_{TT}=0.2\times10^6\text{ psi} \tag{32}$$

E_L and E_T are the Young's moduli, G_{LT} and G_{TT} are the shear moduli, ν_{TT} and ν_{LT} are the Poisson's ratios, and the subscripts L and T denote the directions parallel and normal to the fibers, respectively.

We consider two loading functions

$$q^*=\delta(X)H(T) \tag{33}$$

and

$$q^*=\delta(X)Te^{-T} \tag{34}$$

where $\delta(X)$ and $H(T)$ are the Dirac delta function and the Heaviside function, respectively.

Figure 1 shows the profile of the transverse displacement at $T=1$ in the plate subjected to Type-1 loading given by Eq. (33). The exact displacements at the top surface and at the midplane of the plate are shown in the figure. It is found that the plate solution agrees very well with the exact solution except in the vicinity of the load. In this region, the exact displacements on the top surface ($Z=0.5$) and in the midplane ($Z=0$) also differ substantially. This difference is expected in view of the unboundedness of the stress on the top face under the load.

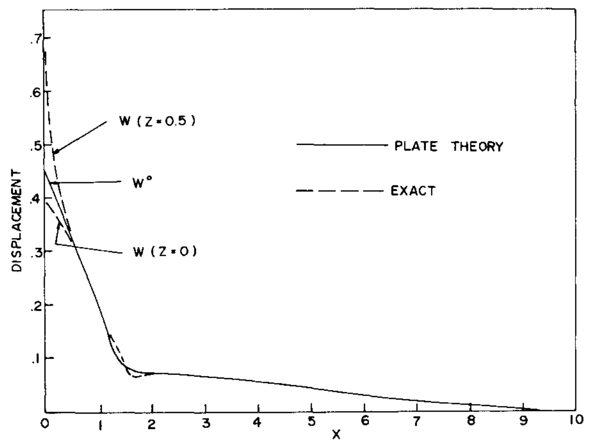

Fig. 1 Displacement profile at $T=1$ for $q^*=\delta(X)H(T)$.

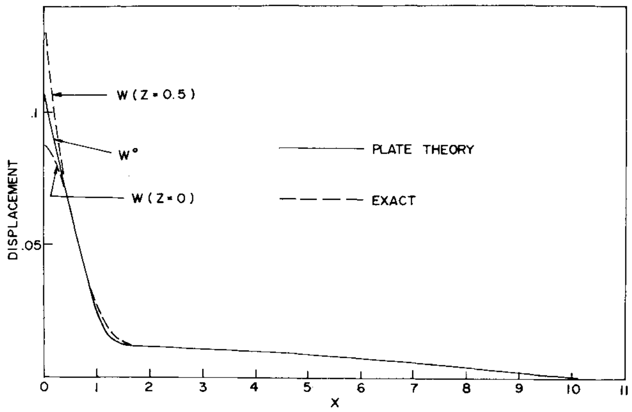

Fig. 2 Displacement profile at $T=1$ for $q^*=\delta(X)Te^{-T}$.

It is clearly observed from Fig. 1 that there are two possible wavefronts propagating. In a recent study on wavefront propagation in laminates,[3] it was found that, in general, there were five possible wavefronts. In the present case there exist two wavefronts according to the results of Ref. 3, namely, the transverse shear wave and the bending wave. The wavefront locations of these two waves which can be read off easily from Fig. 1 were also predicted by Ref. 3. It is noted that at the leading wavefront, which lies at $X\approx9.5$ at $T=1$, there exists a jump in the bending moment, while the second wavefront which occurs at $X\approx1.5$ carries a jump in transverse shear.

The solutions associated with Type-2 loading as given by Eq. (34) are presented in Fig. 2. Because of the relatively smooth application of the load, better agreement between the exact and plate solutions at the wavefront of the transverse shear wave is obtained.

From the present work we can say that the Timoshenko-type plate theories are valid in describing the displacement field for plates subjected to impulsive loadings including even the severe cases such as the loadings represented by a Dirac delta function and a step function.

References

[1] Mindlin, R. D., "An Introduction to the Mathematical Theory of Vibration of Elastic Plates," Monograph prepared for U.S. Army Signal Corps. Engineering Lab., 1955, Fort Monmouth, N.J.

[2] Moon, F. C., "Wave Surface Due to Impact on Anisotropic Plates," *Journal of Composite Materials*, Vol. 6, Jan. 1972, pp. 62–79.

[3] Sun, C. T., "Propagation of Shock Waves in Anisotropic Composite Plates," *Journal of Composite Materials*, Vol. 7, July 1973, pp. 366–381.

[4] Wang, A. S. D., Chou, P. C., and Rose, J. L., "Strongly Coupled Stress Waves in Heterogeneous Plates," *AIAA Journal*, Vol. 10, No. 8, Aug. 1972, pp. 1088–1090.

[5] Whitney, J. M. and Pagano, N. J., "Shear Deformation in Heterogeneous Anisotropic Plates," *Journal of Applied Mechanics*, Vol. 37, No. 4, Dec. 1970, pp. 1031–1036.

[6] Cooley, J. W. and Tukey, J. W., "An Algorithm for the Machine Calculation of Complex Fourier Series," *Mathematics of Computation*, Vol. 90, No. 19, April 1965, pp. 297–301.

[7] Cooley, J. W., Lewis, P. A. W., and Welch, P. D., "The Fast Fourier Transform Algorithm: Programming Considerations in the Calculation of Sine, Cosine and Laplace Transforms," *Journal of Sound and Vibration*, Vol. 12, No. 3, 1970, pp. 315–337.

[8] Brenner, N. M., "Three Fortran Programs That Perform the Cooley-Tukey Fourier Transform," TN 1967–2, July 1967, MIT Lincoln Lab., Cambridge, Mass.